Localized atomic segregation in the spalled area of a $Zr_{50}Cu_{40}Al_{10}$ bulk metallic glasses induced by laser-shock experiment

B Jodar[1], D Loison[1], Y Yokoyama[2], E Lescoute[3], M Nivard[1], L Berthe[4] and J-C Sangleboeuf[1]

[1] Institute of Physics Rennes, UMR CNRS 6251, Rennes, France
[2] Institute for Material Research, Tohoku University, Sendai, Japan
[3] CEA/DAM/DIF, Arpajon, France
[4] PIMM, UMR CNRS 8006, Paris, France

E-mail: benjamin.jodar@univ-rennes1.fr and didier.loison@univ-rennes1.fr

Abstract

Laser-shock experiments were performed on a ternary $Zr_{50}Cu_{40}Al_{10}$ bulk metallic glass. A spalling process was studied through post-mortem analyses conducted on a recovered sample and spall. Scanning electron microscopy magnification of fracture surfaces revealed the presence of a peculiar feature known as cup-cone. Cups are found on sample fracture surface while cones are observed on spall. Two distinct regions can be observed on cups and cones: a smooth viscous-like region in the center and a flat one with large vein-pattern in the periphery. Energy dispersive spectroscopy measurements conducted on these features emphasized atomic distribution discrepancies both on the sample and spall. We propose a mechanism for the initiation and the growth of these features but also a process for atomic segregation during spallation. Cup and cones would originate from cracks arising from shear bands formation (softened paths). These shear bands result from a quadrupolar-shaped atomic disorder engendered around an initiation site by shock wave propagation. This disorder turns into a shear band when tensile front reaches spallation plane. During the separation process, temperature gain induced by shock waves and shear bands generation decreases material viscosity leading to higher atomic mobility. Once in a liquid-like form, atomic clusters migrate and segregate due to inertial effects originating from particle velocity variation (interaction of release waves). As a result, a high rate of copper is found in sample cups and high zirconium concentration is found on spall cones.

Keywords: laser-shock, dynamic behaviour, bulk metallic glasses, shockwave, spallation

(Some figures may appear in colour only in the online journal)

1. Introduction

Unique and intriguing properties of amorphous alloys have nourished several scientific minds during the past few decades. Since their discovery in 1960 by Klement *et al* [1] and their development in bulk glass-form [2], extensive works have been provided on their synthesis, glass forming ability and structure design [3] related to various icosahedral configurations distributions into an amorphous medium depending on the composition. Regarding the mechanical behavior, substantial studies were reported on deformation mechanisms [7] based mostly on the free volume and shear transformation zone (STZ) theories. Cao *et al* [22] used molecular dynamics to correlate the evolution of icosahedral structures under quasi-static loading conditions of a binary Cu–Zr bulk metallic glass (BMG) to the localized shear flow process. Maas *et al* studied experimentally at low strain rates (10^{-3} s^{-1}) the influence of temperature on the shear bands propagation [23] and velocity

[24] to determine how the local structure, that is very temperature sensitive, governs the shear band formation and propagation. Thurneer *et al* [25] performed compression at strain rate between 10^{-4} s^{-1} and 10^{-3} s^{-1} experiments on several compositions of a ternary ZrCuAl BMG at various sub-ambient temperatures to measure the activation energy for shear band propagation and determine how it is linked to atomic bonding.

In contrast, only a few studies were published on the dynamic behavior of BMG. Few equations of states and Hugoniot curves were reported by Martin *et al* on a $Zr_{57}Nb_5Cu_{15.4}Ni_{12.6}Al_{10}$ using single and bi-stage gas guns for pressures up to 122 GPa [8], by Togo *et al* on a $Zr_{55}Al_{10}Ni_5Cu_{30}$ also by plate-impact experiments for pressure range lower than 45 GPa [9] and Xi *et al* on a $Zr_{51}Ti_5Ni_{10}Cu_{25}Al_9$ up to 110 GPa [10]. From these studies, BMG revealed several phases transitions that are composition dependent. The dynamic elasto-plastic transition was previously studied by Turneaure *et al* on a $Zr_{56.7}Cu_{15.3}Ni_{12.5}Nb_{5.0}Al_{10.0}Y_{0.5}$ [11, 12] where the Hugoniot elastic limit (HEL) was measured to be around 7 GPa. The shock wave instability related to pressure just above the HEL highlighted a strain-softening response that is well known in static to be a characteristic response upon loadings exceeding the elastic domain. Smirnov *et al* and Luo *et al* also reported the HEL of a $Zr_{55}AlNiCu$ [14] and a $Zr_{51}Ti_5Ni_{10}Cu_{25}Al_9$ [15] BMG, respectively, to be around 4.5 GPa and 8.9 GPa. Arman *et al* used molecular dynamic simulations to follow the evolution of icosahedral structures on a binary $Cu_{46}Zr_{54}$ BMG for pressure range around the elasto-plastic transition to determine how some icosahedral configurations contribute to strain-softening [13]. The dynamic tensile limits with a strain rate in the range of 10^4 s^{-1} to 10^6 s^{-1} were also reported to be in the range of 2–4 GPa by several authors [16–19] for various Zr-based BMGs, depending on the compositions. The spalling process induced by planar shock and resulting fracture surfaces were also studied. Zhuang *et al* [16] and Yang *et al* [17] performed scanning electron microscopy (SEM) on a recovered target that showed shear band on the cross section and vein-pattern on the fracture surface [6]. Light emission was observed by Sun *et al* during spallation [20]. Escobedo *et al* [19] and Lu *et al* [21] also reported a vein-pattern on the fracture surface that also contained cup-cones formations.

For decades, laser-shock has been used to study spallation in metals [26, 27] and glass [28] but also to study the mixed-mod shock wave loading at high strain rate on polymers [29]. Loadings induced by nanoseconds laser plasma can be reached up to 10^2 GPa with high strain rate (10^6 to 10^9 s^{-1}). This technique with soft low density gel ($\sim$0.9 $g \cdot cm^{-3}$) allows sample and spall recovery for post-mortem analysis [30].The generated loading shape is triangular (1) as illustrated in figure 1. When reaching the rear surface, the shock wave is reflected into a release wave (5). The meeting of the incident and reflected releases engenders an inverted pressure front. Ahead of this front, the specimen is still under compression, while tension is observed behind (close to the free surface). It is essential to notice that the strain rate in compression differs from the one in tension, due to release waves spread. Once the dynamic tensile threshold of the material is reached, spallation occurs, leading to matter separation and ejection (6). Finally, to avoid edge effects in laser shock induced spallation, thin samples are machined to ensure uniaxial strain state.

In this paper, we study spallation at high strain rates and high pressures of a $Zr_{50}Cu_{40}Al_{10}$ BMG using shock produced by laser. Especially, this paper deals with the formation of cup-cone features observed on recovered sample and spall. A discussion focuses on atomic segregation phenomena observed in fracture areas. First part introduces the experimental setup and methods. The second part reports post-mortem observations and measurements. In the last part, results are discussed.

2. Experimental setup

A single master ingot of ternary $Zr_{50}Cu_{40}Al_{10}$ BMG was prepared by arc-melting mixtures of high purity Zr, Cu and Al under an argon atmosphere. The Zr crystal rod used here contains an oxygen concentration less than 0.05 atomic percent to avoid crystallization during casting process. The master ingot was cast using the tilt-casting method [31] into a 10 mm diameter rod and 45 mm long. As reported by Yokoyama *et al* [31], this technique reduces the formation of cold shuts that act as crack-initiation sites. According to initial properties, the density of the $Zr_{50}Cu_{40}Al_{10}$ BMG rod was measured by the Archimedes method using purified water and was found to be 6.809 ± 0.006 $g \cdot cm^{-3}$. The cast structure was also controlled by optical microscopy and SEM and the phase was characterized by x-ray diffractometry exhibiting no Bragg peaks of any crystalline phase. The ultrasonic echography technique was used to obtain Poisson ratios, Young's and shear modulus which were found to be correspondingly equal to 0.369 ± 0.02, 89.3 ± 1 GPa and 32.6 ± 1 GPa. The final target was cut from this single master ingot and polished into a 215 μm thickness slice with a 1 μm flatness controlled by confocal profilometry.

Laser shock experiments were performed on the LULI2000 facility (UMR 7605, Ecole Polytechnique, Palaiseau, France). The laser provides a 4.6 ns duration high power square pulse at 1.06 μm-wavelength focused onto the specimen surface (spot diameter of 2.9 mm). Samples are set in a secondary vacuum chamber (10^{-3} Pa is achieved) to avoid laser breakdown with air. Provided energy is 800 J maximum resulting in laser intensities up to 2.60 $TW \cdot cm^{-2}$. Spalls ejected from target free-surface were collected into a soft recovery device. The experimental setup is displayed in figure 2. Post-mortem observations and analysis were performed on recovered fracture surfaces both on sample and spall by SEM and atomic content was probed by energy dispersive spectroscopy (EDS) on the ScanMat facility (UMS 2001, Rennes, France). Atomic distribution profiles were established in several positions, i.e. in the form of measurements lines made of 200 points with a spatial resolution of 1 μm^3 for each point, to follow the evolution of atomic distribution according to position in cup and cones.

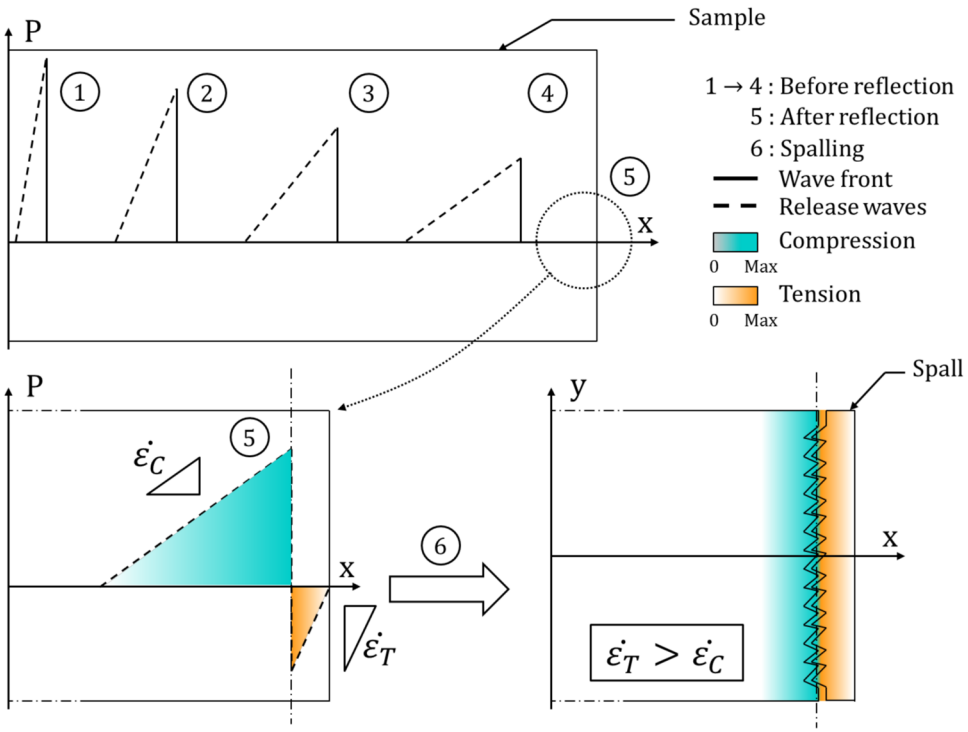

Figure 1. Illustration of a shock wave propagation. Once generated, shock waves induced by laser become triangular (1). During propagation, release waves spread and peak pressure decays with travelled distance (1) → (4). Behind shock front, motion is provided to matter. When arriving at free-surface, the shock wave turns into release waves and pressure drops by the interaction of incident and reflected release waves. Subsequent strain and stress states are no longer compressed but tensed, directly impacting strain rate and inducing loading asymmetry within the specimen. Matter separation (spalling) occurs when the dynamic tensile threshold of the material is reached, resulting in the ejection of matter (spall) (6).

3. Results

Displayed in figure 3 is the typical central spalled area of a 215 μm thick sample (a) irradiated by a 2.45 $\mathrm{TW \cdot cm^{-2}}$ intensity equivalent to a ∼60 GPa pressure obtained by laser-matter interaction simulations using one dimensional Lagrangian code ESTHER [32]. Its corresponding recovered spall is shown in figure 4 (a). First, one may distinguish on both surfaces the presence of multiple objects, referred to as cup-cones. Several authors also reported such a characteristic pattern in the case of plate-impact experiments [19] in a $Zr_{56.7}Cu_{15.3}Ni_{12.5}Nb_{5.0}Al_{10.0}Y_{0.5}$ and [21] in a $Zr_{50}Cu_{40}Al_{10}$ BMG. The main differences between these studies and the present one regards the number, the size, the morphologies but also the location of cup-cones on a spall or sample. Reported cup-cones diameters were on average ten times larger and ten times less numerous for a same area than the one showed here. Lu *et al* [21] reported smoother cup and cones surfaces. Recovered spall and sample surfaces differ from one another respectively from the presence of cups on sample and cones on spall. However, in previous studies spalls were not recovered so that direct confrontation is not possible.

At cup-cones scale, cups emphasize a smooth and viscous-like central region (figures 3(b) and (c), circles in yellow lines). Flat peripheral rings with large vein-pattern can be distinguished (figures 3(b) and (c), circles in blue lines). This vein-pattern is usually observed on fracture surfaces in metallic glasses [6] and results from instabilities in the liquid-like layer that forms during shear banding [5]. Small molten droplets can also be observed (figure 3(c)) mostly in the outlying region, suggesting viscosity drop (or melting). On the contrary, cones appear clearly grainier in the central area (figure 4(b), yellow circle) with fewer or no droplets. The characteristic vein pattern is here thinner than observed on cups central area. Outlying rings with large vein-patterns are sometimes observed on the bottom of cones (figure 4(b), blue circle). According to Deibler *et al* [33], these various vein pattern sizes can be attributed to a viscosity discrepancy, where a large pattern is synonym of low

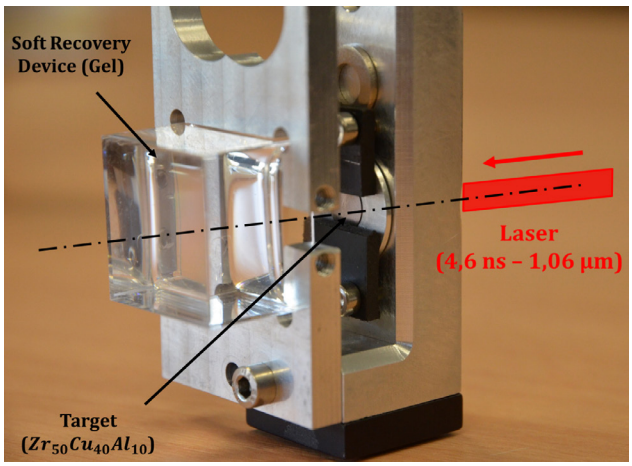

Figure 2. Photograph of the sample holder with the soft recovery device used for collecting ejectas. The complete system is set in a secondary vacuum chamber (10^{-3} Pa is achieved) to avoid laser breakdown with air. In this situation, laser is irradiating the front face of the sample (not visible here) from the right.

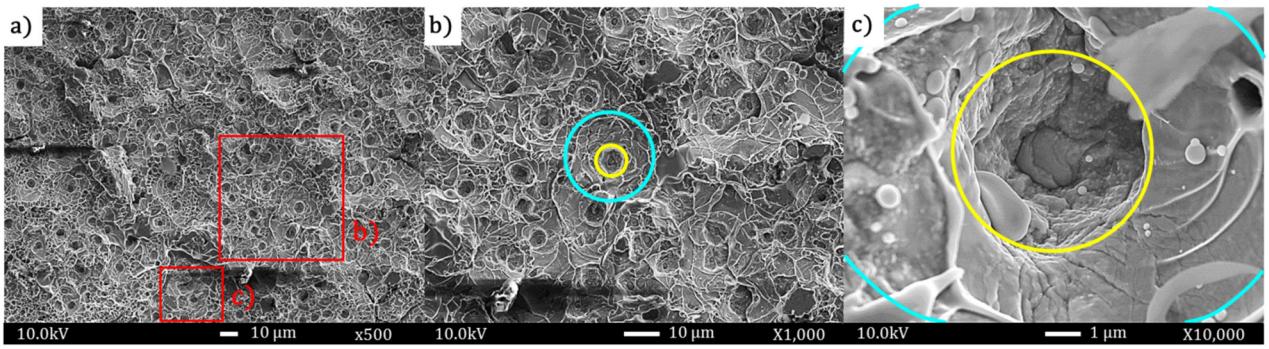

Figure 3. SEM pictures of the recovered sample. Magnifications in picture (a) (squares in red line) reveal a complex fracture surface with cups. Pictures (b) and (c) exhibit two distinct areas on cups: a smooth central area (yellow circle) and a flat outlying one (blue circle). On magnification (c) melted droplets can be distinguished.

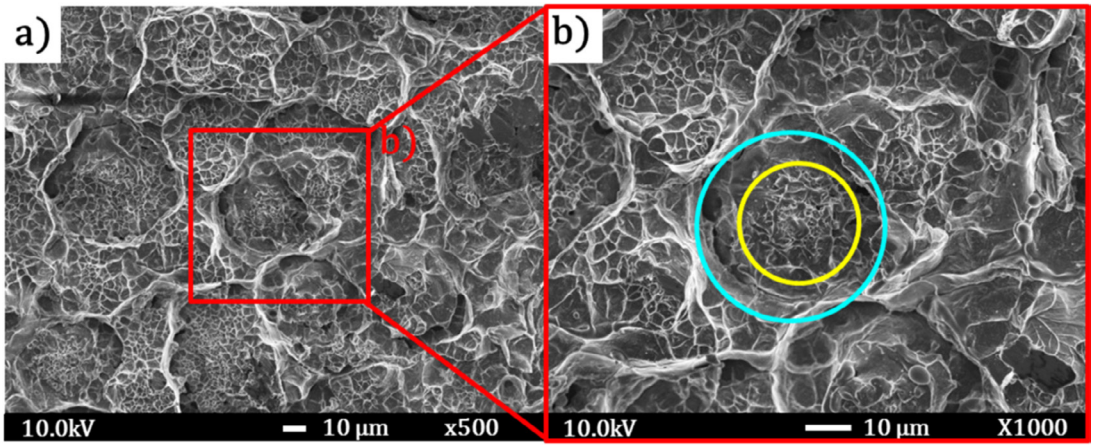

Figure 4. SEM images of the recovered spall. Fracture surface is here made of multiple cones (a). Magnification of image (a) (red square) also emphasized in picture (b) two distinct regions on cones (similar to cups). The smooth central area is depicted by the yellow circle and the flat area by the blue circle.

viscosity, and thin pattern size to high viscosity. This apparent viscosity difference may be explained by Pampillo's work [34] that provided evidence of a structural disordering effect within shear bands. Most specifically, it suggested that chemical potential may be altered relatively to the bulk within the bands. In addition, it was reported by Leamy *et al* [35] that the flow and fracture surface process of metallic glasses in quasi-static tension shows a smooth and a veined regions, similar to the two distinct areas observed both in cups and cones.

At atomic scale, EDS measurements on surfaces of cups (figure 5(a)—red line) and cones (figure 5(b)—red line) revealed atomic composition discrepancies in comparison with the original one (Zr: 50%, Cu: 40%, Al: 10%). Altogether, 50 cups and 50 cones were probed. According to position, atomic distribution in cups (figure 5(e)) and cones (figure 5(f)) varies strongly. By taking account of EDS accuracy ($\pm 5\%$), cups appear rich in copper (Zr: $\sim$25%, Cu: $\sim$70%, Al: $\sim$5%) while cones are rich in zirconium (Zr: $\sim$70%, Cu: $\sim$25%, Al: $\sim$5%). Once outside of these features, atomic content tends to the initial rate, as depicted by figure 5(e).

4. Discussion

In metallic glasses, several studies with quasi-static loadings have provided key elements relative to its plasticity and were regrouped as a deformation map proposed by Schuh *et al* [4]. It is now well established that metallic glasses exhibit two regimes of plastic flows: homogeneous at high temperature and low strain rate, inhomogeneous at room temperature and high strain rate that is associated with shear bands. In this last domain, plasticity and yielding are controlled by the initiation, the propagation and the evolution of shear bands that usually lead to failure.

In the present study, i.e. in a dynamic loading situation, strain rate is very high and temperature remains an open question. Nonetheless, according to shock wave nature (that is strongly discontinuous), it is presumably reasonable to consider that plastic flow under shock is inhomogeneous. With this in mind, initiation and propagation of cup-cones correlated with a process for atomic segregation will be discussed according to the shock wave theory but also results reported by quasi-static studies on metallic glasses.

4.1. Cup-cone initiation and propagation

If one considers a peculiar site from which plasticity can be initiated (figure 6(1)), when the shock wave (schematized by the blue front traveling from left to right) interacts with this site, a surrounding displacement field is induced. This local atomic displacement is larger than the one of the surrounding

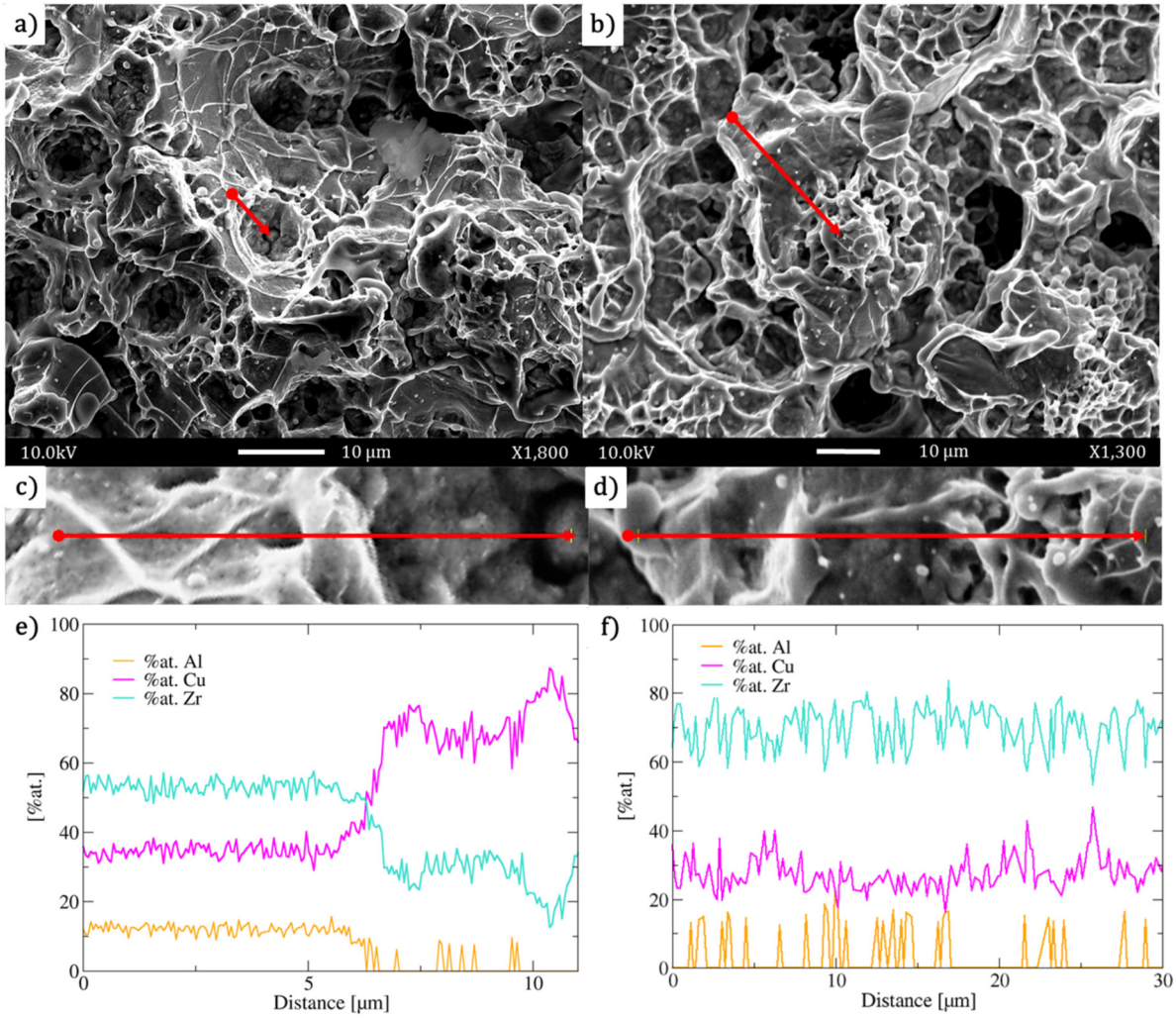

Figure 5. EDS measurements of atomic distribution on cup-cones fracture surface. SEM magnifications of sample cups (a) cones on recovered spall (b) with the probed positions (red lines). Magnifications of probed cup and cone are depicted by red lines in (c) and (d), respectively. The atomic distribution of Zr, Cu and Al depending on the position is displayed for a cup (e) and a cone (f). Cups seem to be rich in copper and poor in zirconium. It is the opposite for cones that are rich in Zr and lack Cu. Aluminum content remains approximately constant. Outside of the cup-cone feature, the initial composition rate is found.

matrix leading to local shearing. This region of local atomic displacement and shearing has been referred to in the literature as shear transformation [36] or STZ [37] and is assumed to be responsible for plasticity triggering. Experimental [38] and numerical [39] studies emphasized the quadrupolar character of the created strain field (red areas in figure 6) which decays with the distance from the STZ center to the surrounding matrix (figure 6(1)). Greer *et al* [5] proposed a two-stage scenario for shear band initiation. Once a STZ is activated (first stage) the atomic structure is disordered and atoms gain mobility.

At that point, shear strain is small and temperature rise not substantial. Hence, it forms a softened path for sliding and shear to concentrate (second stage). Since matter is softened along a privileged path, large plastic strain accumulates and localizes to form a shear band. From this localization, significant local heating results thanks to the thermodynamics equation.

In the present case, an initiation site is firstly activated by the arrival of the compression front and it engenders atomic disorder in a quadrupolar way, as is illustrated by steps (1) → (2) in figure 6. Since there is no clear evidence that cup-cones originate from STZ triggering, we rather consider any sort of sites from which shear strain may concentrate. The shock- and release waves rarefaction turning the compression into tension triggers the second stage where shear bands initiates (3) → (4). Once the spallation plane is reached, shear bands on the right are fully formed and sliding begins (5). Finally, when crack initiates, it propagates along softened paths described by fully developed shear bands on the right side. In addition, in the central spot area the strain state is uniaxial (due to initial loading conditions). From this uniaxial strain state and the quadrupolar form of shear concentration, results the formation of cups on samples and cones on spall. According to smooth and vein-pattern areas observed both on cups and cones, one may consider the temperature evolution during sliding. While sliding, temperature may rise until possibly reaching melting point. At the early stage of sliding, temperature is lower (high viscosity) than at later stages (low viscosity). Therefore, it conducts to the formation of two distinct areas on cup and cones fracture surface.

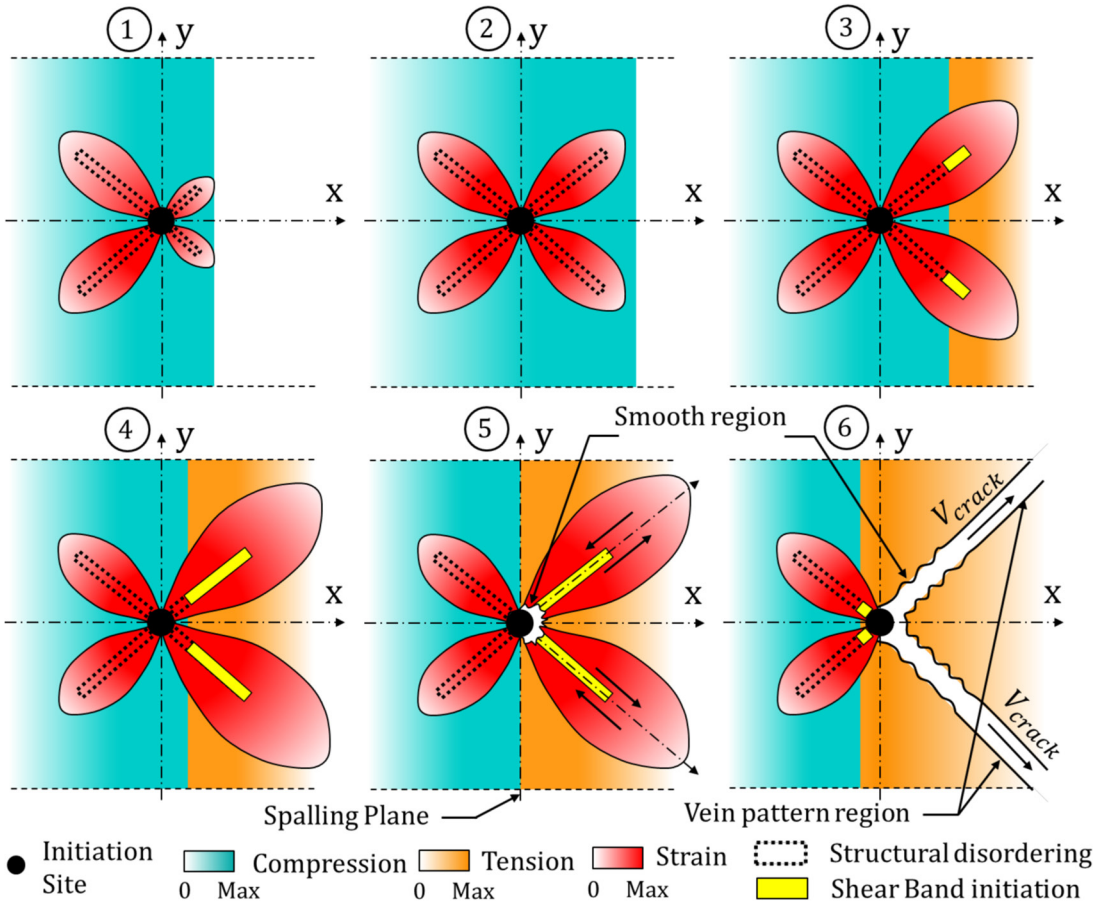

Figure 6. Schematic representation of sites initiation kinetic during shock wave propagation and reflection leading to cup-cone pattern generation. In compression phase (1) → (2), a shock wave induces a displacement field that disorders atomic structure locally and activates an initiation site. Matter is softened along a band. After rarefaction, tension occurs and large plastic strain accumulates within the disordered band and engenders the formation of shear bands (3) → (4). At the spallation plane, matter starts sliding and cracks follow softened paths resulting from the shear band's complete formation (5). Then a cup and cone feature is created. During sliding, temperature evolution modifies viscosity within bands so that two distinct areas can be observed on fracture surface: smooth and vein-pattern (6).

4.2. Atomic segregation process

Atomic segregation pointed out by EDS measurements may be the result of a segregation that takes place during shear banding events. Thermodynamically, a shock wave is considered as an adiabatic transformation that induces a jump of pressure and a decrease in volume resulting in a gain of free energy and temperature. Then, localized plasticity responsible for cups and cones formation from initiation sites (metallurgical defect, free volume or STZ) also contributes to temperature and free energy elevation. This temperature rise (or free energy) is responsible for the drop of viscosity (glass transition or melting) allowing atomic mobility within a softened local neighborhood. Once the matter is locally in a liquid-like state along with the particle motion provided by a shock wave, atoms could migrate. Since our material is made of various compounds possessing different masses (Zr: 91u, Cu: 63u, Al: 27u) inertial effects could emerge.

For an identical particle velocity, Zr atoms possess more kinetics energy than Cu and Al. Hence, segregation would take place during a phase of velocity decrease, where Cu and Al atoms would decelerate more rapidly than Zr atoms. To understand how such a scenario could happen, one may refer to figure 7 illustrating the variation of pressure and particle velocity during reflection and overlapping.

In early stages, matter is being compressed by the shock wave propagation that induces pressure, temperature and velocity jump. Once the shock wave reaches the free-surface, reflection occurs and the particle velocity rises (more or less doubled) while pressure drops to zero and temperature decreases (but stays higher than the initial one). By overlapping at spallation plane, incident and reflected releases modify particle velocity substantially. Hence, the particle velocity increases at a velocity u_{t1} and tensile stresses result from overlapping. Assuming a stress level above a tensile threshold σ_T (relative to plasticity activation, i.e. shear band initiation), localization and viscosity drop take place soon after t_1 and promote migration. Taking account of hydrodynamic damping and release waves spreading, particle velocity decreases to u_{t2} at t_2. As a result, the particle velocity u_{t2} at t_2 is below u_{t1} at t_1. In short, after reaching σ_T the current viscosity drops (see section 4.1) and particle velocity rises to u_{t1} resulting in a motion of atomic clusters. A little while after, particle velocity decreases to u_{t2} and inertial effects are forecast to happen due to atomic mass differences: Cu and Al are slowed and Zr atoms continue on their path. This hypothesis is sufficient to

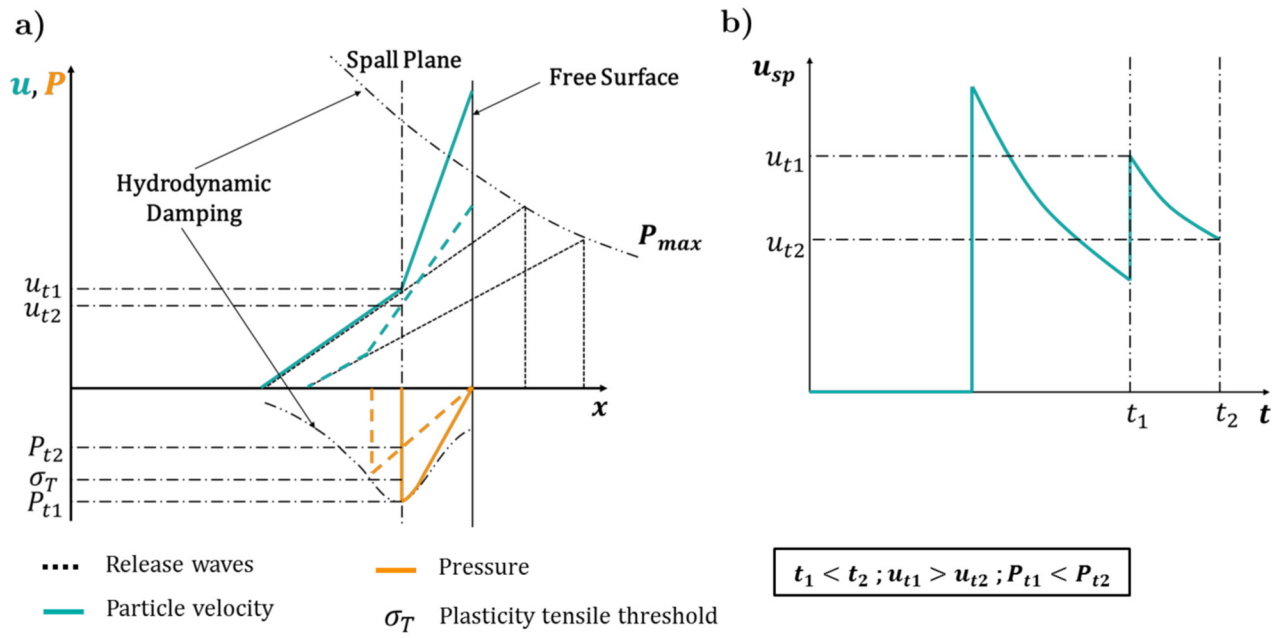

Figure 7. Illustrations of shock wave propagation and reflection inducing pressure and particle velocity changes. In schema (a) particle velocity and pressure versus position are plotted. In schema (b) the particle velocity at spall plane during time is plotted.

understand why high Zr and Cu rates are respectively found on spall and sample fracture surfaces but not enough to explain the aluminum constant rate on both surfaces.

According to the molecular dynamic simulations of Cheng *et al* [40] on a $Zr_{47}Cu_{46}Al_7$ showing partial differential functions for these compounds, Cu–Al and Zr–Al are the strongest bonds. Then, Cu–Zr, Cu–Cu and finally Zr–Zr bonds are the weakest. Assuming that Cu–Al and Zr–Al are highly energetic compared to other bonds and that cracks propagate along paths minimizing energy, one may suggest that during separation, cracks would neglect as much as possible these bonds areas. Thus, only Cu–Cu, Zr–Zr and Cu–Zr bonds remain. Since Al atoms are the lighter but also strongly bonded to Cu and Zr, our results seem to suggest that cracks split mostly Cu–Zr bonds during or after the segregation phenomenon.

Regarding morphology, the composition segregation is possibly responsible for the cups and cones aspects. Zirconium possesses the highest melting temperature of the three: $T_{Zr} = 2130$ K, $T_{Cu} = 1350$ K, $T_{Al} = 933$ K. Furthermore, Yokoyama *et al* [41] showed that Zr-rich ternary ZrCuAl (for a fixed value of Al) possesses the highest melting temperatures. Hence, for a fixed temperature, areas highly concentrated in zirconium will show a higher viscosity than Cu-rich areas. This is clearly in agreement with our observation but also with the correlation of vein pattern size and viscosity level exposed by Deibler *et al* [33].

5. Conclusion

In summary, the spalling process induced by a laser has been studied on a $Zr_{50}Cu_{40}Al_{10}$ BMG. Post-mortem analyses were conducted on a recovered sample and spall. SEM images revealed the presence of cups (on sample) and cones (on spall) featuring various morphological aspects. Two distinct regions can be observed both on cups and cones: a smooth viscous-like region in the center and a flat one with large vein-pattern in the periphery. EDS measurements performed on the fracture surface exhibited an atomic segregation that could take place during spallation. Cups appear rich in copper while cones are rich in zirconium. Outside of these features the initial composition rate is found.

Atomic migration and segregation took place at the spallation plane into the shear band initiation. On one hand, a viscosity drop resulting from temperature increase and atomic disorder would favor atomic mobility. On the other hand, shock and release waves propagation and interaction engender particle velocity variations. These two aspects promote atomic segregation through inertial effects.

The initiation and the propagation of cups and cones result from shear bands initiation and asymmetrical loading conditions at the spalling plane, induced by shock wave rarefaction. Shear bands initiation originates from a quadrupolar-shaped atomic disorder, firstly engendered by the compression front that would turn into shear bands when tensile front reaches spallation plane. During the separation process, cracks arise from shear bands (softened paths) and creates cups and cones features.

Acknowledgments

The authors express their gratitude to all the LULI and SCANMAT staffs for technical support. The access to the LULI facility was provided through the Institute Laser Plasma (ILP, FR2707). This work was supported by DGA and ARED grants.

References

[1] Klement W, Willens R and Duwez P 1960 *Nature* **187** 869
[2] Inoue A 2000 *Acta Mater.* **48** 279
[3] Wang W, Dong C and Shek C 2004 *Mater. Sci. Eng.* R **44** 45
[4] Schuh C A, Hufnagel T C and Ramamurty U 2007 *Acta Mater.* **55** 4067
[5] Greer A L, Cheng Y Q and Ma E 2013 *Mat. Sci. Eng.* R **74** 71
[6] Sun B and Wang W 2015 *Prog. Mater. Sci.* **74** 211
[7] Hufnagel T, Schuh C and Falk M 2016 *Acta Mater.* **109** 375
[8] Martin M, Sekine T, Kobayashi T, Kecskes L and Thadhani N 2007 *Metall. Mater. Trans.* A **38A** 2689
[9] Togo H, Zhang Y, Kawamura Y and Mashimo T 2007 *Mater. Sci. Eng.* A **449–51** 264
[10] Xi F, Yu Y, Dai C, Zhang Y and Cai L 2010 *J. Appl. Phys.* **108** 083537
[11] Turneaure S, Winey J and Gupta Y 2004 *Appl. Phys. Lett.* **84** 1692
[12] Turneaure S, Winey J and Gupta Y 2006 *J. Appl. Phys.* **100** 063522
[13] Arman B, Luo S N, Germann T and Çağin T 2010 *Phys. Rev.* B **81** 144201
[14] Smirnov I, Atroshenko S, Sudenkov Y, Morozov N, Zheng W, Naumova N and Shen J 2012 *AIP Conf. Proc.* **1426** 1121
[15] Luo B, Wang G, Tan F, Zhao J, Liu C and Sun C 2015 *AIP Adv.* **5** 067161
[16] Zhuang S, Lu J and Ravichandran G 2002 *Appl. Phys. Lett.* **80** 4522
[17] Yang C, Liu R, Zhan Z, Sun L and Wang W 2006 *Mater. Sci. Eng.* A **426** 298
[18] Yuan F, Prakash V and Lewandowski J 2009 *Mech. Mater.* **41** 886
[19] Escobedo J and Gupta Y 2010 *J. Appl. Phys.* **107** 123502
[20] Sun B-R, Zhan Z J, Liang B, Zhang R J and Wang W K 2011 *Chin. Phys. Lett.* **28** 096102
[21] Lu L, Wang W, Zhu M, Gong X and Luo S 2016 *Mater. Sci. Eng.* A **651** 848
[22] Cao A, Cheng Y and Ma E 2009 *Acta Mater.* **57** 5146
[23] Maaß R, Klaumünzer D and Löffler J 2011 *Acta Mater.* **59** 3205
[24] Maaß R, Klaumünzer D, Villard G, Derlet P and Löffler J 2012 *Appl. Phys. Lett.* **100** 071904
[25] Thurnheer P, Maaß R, laws K, Pogatscher S and Löffler J 2015 *Acta Mater.* **96** 428
[26] Cottet F and Boustie M 1989 *J. Appl. Phys.* **66** 4067
[27] Boustie M and Cottet F 1991 *J. Appl. Phys.* **69** 7533
[28] de Rességuier T and Cottet F 1994 *EURODYMAT 4th Int. Conf. on Mechanical and Physical Behaviour of Materials under Dynamic Loading (Oxford, UK, 26–30 September); J. Phys.* IV *France* **4** 629
[29] Jajam K C and Sottos N C 2016 *J. Dyn. Behav. Mater.* **2** 379
[30] Lescoute E, Rességuier T D, Chevalier J M, Boustie M, Cuq-Lelandais J P and Berthe L 2009 *Appl. Phys. Lett.* **95** 211905
[31] Yokoyama Y, Kobayashi A, Fuhaura K and Inoue A 2002 *Mater. Trans.* **43:3** 571
[32] Colombier J, Combis P, Bonneau F, Harzic R L and Audouard E 2005 *Phys. Rev.* B **71** 165406
[33] Deibler L and Lewandowski J 2012 *Mater. Sci. Eng.* A **538** 259
[34] Pampillo C 1972 *Scr. Metall.* **6** 915
[35] Leamy H, Chen H and Wang T 1972 *Mater. Trans.* **3** 699
[36] Argon A 1979 *Acta Metall.* **27** 47
[37] Falk M and Langer J 1998 *Phys. Rev.* E **57** 7192
[38] Schall P, Weitz D and Spaepen F 2007 *Science* **318** 1895
[39] Tanguy A, Leonforte F and Barrat J L 2006 *Eur. Phys. J.* E **20** 355
[40] Cheng Y Q, Ma E and Sheng H W 2009 *Phys. Rev. Lett.* **102** 245501
[41] Yokoyama Y, Ishikawa T, Okada J T, Watanabe Y, Nanao S and Inoue A 2009 *J. Non-Cryst. Solids* **355** 317